Medicinal Chemistry Research (2019) 28:2218–2231
https://doi.org/10.1007/s00044-019-02448-9

MEDICINAL CHEMISTRY RESEARCH

ORIGINAL RESEARCH

Acetone effects on *Buddleja scordioides* polyphenol extraction process and assessment of their cellular antioxidant capacity and anti-inflammatory activity

Cecilia Villegas-Novoa[1] · José A. Gallegos-Infante[1] · Rubén F. González-Laredo[1] · Alejandro M. García-Carrancá[2] · Karen M. Herrera-Rocha[1] · Janett S. Jacobo-Karam[3] · Martha R. Moreno-Jiménez[1] · Nuria E. Rocha-Guzmán[1]

Received: 24 July 2019 / Accepted: 17 September 2019 / Published online: 28 September 2019

Abstract

The use of water, acetone, and hydroacetonic solutions as an extraction solvent for polyphenol compounds from *Buddleja scordioides* has been investigated. The phenolic profiles determined by liquid chromatography—electrospray ionization—mass spectrometry/mass spectrometry (LC–ESI–MS/MS) were compared with those obtained with the traditional aqueous infusion used for the treatment of gastrointestinal disorders. It was evaluated the effects of polyphenol extract at physiologically relevant conditions against H_2O_2-induced oxidative stress via attenuation of reactive oxygen species (ROS) levels and lipopolysaccharide (LPS)-induced inflammation in human HT-29 cells. The use of hydroacetonic solutions allows obtaining phytochemical extracts enriched with constituents that have antioxidant and anti-inflammatory activity in intestinal cells. This suggests that polyphenols of low and middle polarity from *Buddleja scordioides* may be better extracted with hydroacetonic solutions, and showing high nutraceutical potential to reduce oxidative stress associated with the onset and progress of inflammatory diseases.

Keywords *Buddleja scordioides* · Polyphenols · Antioxidant · Anti-inflammatory activity

Introduction

Inflammation of the colon is an important pathology due to its capacity to promote the development of cancer. Colitis can be caused by different factors, one of the most studied for its importance in public health is the inflammation caused by bacterial infection. Gram-negative bacteria contain endotoxins in their outer membrane called lipopolysaccharide (LPS). Bacterial LPS induces the inflammatory response through the activation of toll-like receptors 4 and several intracellular signaling pathways downstream. When the intestinal epithelial cells are in contact with LPS, the NF-κB p65 is separated from IκB and translocated to the nucleus to regulate the expression of inflammatory mediators. The inflammation pathways activated by LPS include MAPK, Akt1, and activation of NF-κB, which are related to inflammatory bowel disease (IBD) (Seyedabadi et al. 2018). The molecular response in a bacterial infection is through phosphorylation and activation of the expression and synthesis of chemokines such as IL-8, interleukins for example IL-1β, IL-6 and IL-12, and the cytokine TNF-α. During bacterial invasion in epithelial cells, IL-8 participates in the attraction of neutrophils, immature dendritic cells, and natural killer cells that are responsible for restoring cellular homeostasis. In inflammation, some cytokines such as IL-8 and TNF-α are important activators

✉ Martha R. Moreno-Jiménez
mrmoreno@itdurango.edu.mx

✉ Nuria E. Rocha-Guzmán
nrocha@itdurango.edu.mx

[1] Research Group on Functional Foods and Nutraceuticals. Departamento de Ingenierías Química y Bioquímica, TecNM/ Instituto Tecnológico de Durango, Felipe Pescador 1830 Ote., 34080 Durango, Dgo., México

[2] Laboratorio de Virus y Cáncer, Unidad de Investigación Biomédica en Cáncer, Instituto de Investigaciones Biomédicas, Universidad Nacional Autónoma de México, Instituto Nacional de Cancerología, Secretaría de Salud, Av. 12 San Fernando 22, Col. Sección XVI, 14080 Del Tlalpan, CDMX, México

[3] Facultad de Medicina y Nutrición, Universidad Juárez del Estado de Durango, Av. Universidad y Fanny Anitúa s/n, 34000 Durango, Dgo., México

of the acute phase (Matsumoto et al. 2018), causing an increase in the concentration of interleukins; when the concentration is high enough, the cytokines enter the blood circulation and act as endogenous pyrogens causing fever, the main symptom of IBD caused by bacteria. Once the disease is active, there is secretion of a large number of inflammatory mediators including histamine, leukotrienes, amyloid A protein, and prostaglandins. Prostaglandins are derived from the oxidation of arachidonic acid, which is catalyzed by cyclooxygenase enzymes. The cyclooxygenase gene codes for COX-1 and COX-2 isoenzymes. In colon, COX-1 modulates mucosal synthesis and pH stability, besides it prevents the contact of bacteria with epithelial cells. During normal conditions, COX-2 is detectable at low expression or undetectable. The expression of COX-2 results in increase of prostaglandins, which act as inflammation markers. During bacterial infections, COX-2 can be induced by LPS, via activation of the transcription factor NF-κB and by oxidative stress caused by the activity of immune system cells (Li et al. 2018). Due to this contrast of responses, COX-2 is used as a marker of inflammation in bioactivity studies of candidate compounds for inflammation treatment therapies. In this context, nonsteroidal anti-inflammatory drugs are the main treatments for the inhibition of cyclooxygenases due to their clear inhibitory effect. However, these drugs are known for their severe side effects caused by the nonspecific inhibition of COX (Mattia and Coluzzi 2005), inhibiting both COX-1 and COX-2 cyclooxygenases, both important for the homeostasis of the intestinal mucosa.

Several species of the genus *Buddleja* have been reported with pharmacological activities. Particularly, *B. scordioides* traditionally known as salvilla, is a branched, aromatic plant endemic to Mexico, which has been widely used in traditional medicine. Infusions of its leaves have shown antioxidant, anti-inflammatory, hepatoprotective, and gastroprotective activities (Díaz-Rivas et al. 2015), as well as inhibitory effect of lipid peroxidation (Rocha-Guzmán et al. 2018). Phytochemical studies of this plant indicate the presence of flavonoids, iridoids, phenylpropanoids, sesquiterpenes, and saponins (Avila and Romo de Vivar 2002; Díaz-Rivas et al. 2018). Particularly, flavonoids are closely linked to various biological activities, highlighting flavonols and flavones subclasses. Quercetin is considered the most active antioxidant of the subclass of flavonols (Atala et al. 2017) and luteolin of the subclass of flavones (Choi et al. 2014). The flavonoid antioxidant characteristic is associated with its dihydroxy functionality in carbons 2 and 3 of the B ring (i.e., catechol ring) that confers to the molecule lower energy requirement for the electron and hydrogen transfer mechanisms (Leopoldini et al. 2004). These flavonoids, in addition to being recognized for their antioxidant activity, are widely documented for their vasodilator and anti-inflammatory effects (Psotová et al. 2004; Mueller et al. 2010). Consequently, the process of separation and purification is a crucial step in the procedures of extracting nutraceuticals from this source.

Nutraceuticals are recognized as concentrated formulas of bioactive compounds with biological effects scientifically proven, for the prevention or treatment of certain diseases. These products include isolated nutrients, dietary supplements, and herbal products. The development of nutraceuticals implies validation of the health allegations attributed to them. These products represent different types of businesses and markets, and their consumption is mostly related to a healthy lifestyle. Consumers who have previously been dependent on dietary supplements are switching to nutraceuticals in the category of nutrients, vitamins, minerals, botanicals, and herbs.

The trend indicates that maintaining a healthy digestive and immune systems is considered a priority in the consumption of these products. In such a way that research on natural products with therapeutic potential, represents an area of great interest in herbal products, which have been the most important source. Among the methods that are currently used to obtain nutraceuticals are thin-layer chromatography and column chromatography, although they are methodologies that require longer times of processing. A method recently used for the separation of flavonoids is through the use of molecularly imprinted polymers, which are imitators of antibodies made by man (Bai et al. 2018); however, these templates are still expensive and have little practical use when handling polar solvents such as water (Pakade et al. 2012). In this regard, the use of conventional approaches for obtaining extracts enriched with anti-inflammatory compounds is a goal. Among the organic solvents used in traditional methods of extraction of nutraceuticals is acetone. Some studies indicate that extractables of acetone obtained from various sources, show antiproliferative activity of gastric cancer cells (Yang et al. 2018) and breast cancer cells (Tanih and Ndip-Ndip 2017). Few studies have explored the effect of hydroacetonic solutions for the enrichment of extracts with anti-inflammatory activity. Hence, this study was conducted to examine the antioxidant and anti-inflammatory effect of a nutraceutical extract rich in flavonols and flavones extracted from *Buddleja scordioides* with aqueous and hydroacetonic solutions.

Material and methods

Plant material

Salvilla plants (*Buddleja scordioides*) were collected on August 2016 in José Guadalupe Rodríguez, Durango, Dgo., México (24°18′58.5′′N, 104°05′02.6′′W), and botanically identified with voucher number 47538 by Dr Socorro

González-Elizondo at the CIIDIR-IPN Herbarium. *B. scordioides* plants were dried at room temperature and milled to powder form before use.

Reagents and biological materials

The HT-29 cells were obtained from the American Type Culture Collection. Quinic acid, protocatechuic acid, chlorogenic acid, 2,5-dihydroxybenzoic acid, 4-hydroxybenzoic acid, 4-O-caffeoylquinic acid, vanillic acid, caffeic acid, coumaric acid, ferulic acid, rosmarinic acid, rutin, quercetin-3-O-glucoside, quercetin-3-O-glucuronide, hesperidin, luteolin, quercetin, apigenin, naringenin, acacetin, MTT (3-[4,5-dimethylthiazol-2-yl]-2,5, -diphenyl-2-tetrazolium bromide), and DMSO (dimethyl sulfoxide), H_2DCF-DA, RPMI-1640 medium, trypsin, penicillin G, and streptomycin sulfate were obtained from Sigma Chemical (St. Louis, MO, USA), fetal bovine serum (FBS) was obtained from Bio-West (Kansas City, MO, USA) and LPS from *Escherichia coli* (serotype 0111: B4; Sigma-Aldrich, MO, USA). Deionized water was purified by Milli Q Water Purification system from Millipore (Millipore Corp., Bedford, MA); acetone and acetonitrile LC–MS grade were from J. Baker. All other reagents (chemical and solvents) utilized were analytical grade and purchased from standard commercial suppliers.

Preparation of extracts

One percent (w/v) water extracts (infusion—*Inf*) were prepared using dried *B. scordioides* and distilled water maintained at 80 °C for 10 min in a hot water bath (Felisa, Fabricantes Feligneo, Jalisco, México). Infusions were cooled off at room temperature and centrifuged at 4500 rpm. The supernatants were filtered through Whatman filter paper No. 1 and the filtrates frozen and lyophilized in a freeze dryer (Labconco 18L, Kansas, M.O.).

Buddleja scordioides powder (425 µm) was extracted (*EAc*) with acetone 100% and hydroacetonic solutions [70, 75, 80, 85, 90, and 95% of acetone] by homogenization (24,000 rpm) with an ultra-turrax® IKA®T10 basic system using three cycles of sonication of 15 and 45 s on ice, the samples were centrifuged at 4500 × *g* for 10 min with a centrifuge Labofuge 400R Heraeus, U.S. The supernatant was recovered and the process repeated twice. Finally, the total extract solution was evaporated at 40 °C using a rotary vacuum evaporator; the recovered powder was resuspended in milli Q water and then lyophilized.

Chemical characterization

Sample analysis was carried out with an Acquity UPLC system (Waters Corp., Milford, MA, USA) coupled with a tandem Xevo TQ-S triple quadrupole mass spectrometer (Waters Corp., Milford, MA, USA). The LC system consisted of a sample manager (6 °C) and a quaternary solvent manager. Phenolic compounds were detected with an Acquity UPLC BEH C18 100 mm × 2.1 mm × 1.7 µm column (Waters Corp., Milford, MA, USA), operated at 40 °C. The elution profile included two solvents, acidified water with 7.5 mM formic acid (A) and acetonitrile LC–MS grade (B): initial 97% A; 1.23 min, 91% A; 3.82 min, 84% A; 11.40 min, 50% A; 13.24 min, 97% A and 15.0 min, 97% A. MRM data were collected from 0 to 16.0 min. Flow rate was of 210 µL min^{-1} and ionization was carried out using as cosolvent methanol with 0.1% of formic acid (v/v) at a flow of 5 µL min^{-1} with the use of an isocratic solvent manager (Waters Corp., Wexford). Detection of the main flavonoids present in *B. scordiodes* was performed by LC–PDA, and the identification of these compounds was confirmed by ESI–MS/MS in multiple reaction-monitoring mode. Negative ionization mode was used for MS assays. MS conditions were as follows: capillary voltage, 3.0 kV; cone, 30 V; desolvation temperature 400 °C, source temperature, 150 °C; desolvation and cone gas flow, 800 and 150 L h^{-1}, respectively; nebulizer gas flow, 7.0 Bar and collision gas, 0.13 mL min^{-1}. A mixture of different phenolic standard compounds was used to monitor retention time and *m/z* values. For quantification of phenolic compounds, calibration curves were done. The UPLC and tandem Xevo TQ-S triple quadrupole mass spectrometer control and data processing were performed using MassLinx software (Waters Corp., Milford, MA, USA).

Theoretical determination of solubility

The contribution level of the chemical groups for the prediction of enthalpy and melting temperatures were obtained following the methodology of Marrero and Gani (2001), while the terms related to the contribution of the functional groups with the surface area and their volumes was carried out using the modified UNIFAC method reported by Theo et al. (2016). The solubility in mixtures was determined by the method proposed by Zhang et al. (2015). The magnitude of deviation of the predicted solubility with respect to the theoretical solubility was carried out by means of literature search on the solubility in water and acetone of quercetin (Chebil et al. 2010), rutin (Zi et al. 2007), vanillic acid (Zhang et al. 2015), and isoquercetrin (Chebil et al. 2010), in all cases the maximum error observed was <10%.

Cell culture

Human colorectal adenocarcinoma cells HT-29 were grown in RPMI-1640 medium supplemented with 10% (v/v) FBS, 100 µg mL^{-1} streptomycin sulfate, 100 U mL^{-1} penicillin G, and cultured in a 37 °C humidified atmosphere

containing 5% CO_2. Cells at preconfluence were used for all assays. The lyophilized extracts were assayed in cell cultures; to do so, they were dissolved in DMSO by sonication to a concentration of 300 mg mL^{-1}. Just before treatments, extracts were dissolved in the culture medium to the required final concentrations ensuring that the maximum DMSO concentration in medium was <0.04%. DMSO without *B. scordioides* extracts was used as control.

Cell cytotoxicity (MTT Assay)

The MTT assay was conducted to determine the optimum concentration of *B. scordioides* for subsequent cell treatments. Cell mitochondrial enzymatic activity was assayed by the 3-[4,5-di-methylthiazol-2-yl]-2,5-diphenyl-2-tetrazolium bromide, as an indirect measurement of cell viability for cytotoxicity determinations. Cells were seeded at an initial density of 9.6×10^3 cells $well^{-1}$ in 96-well plates with RPMI-1640 culture medium, grown for 72 h, and treated with *Inf* and *EAc* of *B. scordioides* extracts for 24 h tested at six final concentrations (30, 100, 250, 1000, 2500, and 5000 ng mL^{-1}) for extracts dissolved in FBS-free medium. All controls were kept to a maximum concentration of 0.04% of DMSO. Assays were carried out to analyze the cytotoxicity for each extract and determine the concentration to be used in later assays. Cells were treated with extracts for 24 h after each well was washed twice with phosphate-buffered saline (PBS) to remove extract residues. MTT solution (1 mg mL^{-1} stock) was added to cells, and incubation continued for 4 h at 37 °C. The formazan crystals produced in living cells were dissolved in 200 µL of DMSO. Absorbance was read at 570 nm (measurement) and 690 nm (reference) using a 96-well plate ELISA reader (Synergy HT microplate reader, Biotek, USA).

Effect of *B. scordioides* extracts on H_2O_2-induced intracellular oxidative stress

HT-29 cells (1.5×10^6 cells $plate^{-1}$) were incubated at a final concentration of 100 ng mL^{-1} with or without *Inf* and *EAc* separately for 24 h to analyze the effect of *B. scordioides* on reactive oxygen species (ROS) reduction. Pretreated HT-29 cells were detached with trypsin 0.15% and incubated at 400 µM of H_2O_2 for 1 h, after then cells were incubated with 5 µM H_2DCF-DA at 37 °C for 30 min, washed twice with ice-cold PBS, and collected by centrifugation at 2000 *g* for 5 min to remove extracellular H_2O_2. Cells were then resuspended in 10 mM PBS–HEPES and transferred into 5 mL round-bottom polystyrene tubes with cell-strainer caps. Tubes were protected from light until ready for analysis. H_2DCF-DA, a nonfluorescent substance, passively diffuses into cells and is deacetylated by esterases to form nonfluorescent 2′,7′-dichlorofluorescein (H_2DCF), which is further oxidized by ROS to fluorescent dichlorofluorescein (DCF), which is trapped inside the cells and can be quantified by flow cytometry. The fluorescence intensity was determined using flow cytometer (S3e™ Cell Sorter, Bio-Rad, USA) with excitation and emission wavelengths of 488 and 525 nm, respectively. The mean fluorescence peak was analyzed from the gated cell population of 10,000 events.

Total RNA extraction and reverse transcription

HT-29 cells were treated with or without *Inf* and *EAc* separately for 24 h, and then cells were treated with 10 ng mL^{-1} LPS from *E. coli* (serotype 0111: B4). The total RNA for detection on pro-inflammatory mediators was extracted at 6 h after LPS-stimulation. Total RNA was isolated from HT-29 cells by SV Total RNA Isolation System (Promega, Madison, WI, USA) according to the manufacturers' protocol. RNA quality was evaluated by visualizing the 28S/18S ribosomal RNA on denaturing agarose gel to 1% containing Diamond™ nucleic acid dye and visualized by UV transillumination (ChemiDoc™, Bio-Rad, USA). The yield of total RNA obtained was determined spectrophotometrically at 260 nm, where one absorbance unit (A_{260}) equals 40 µg of single-stranded RNA mL^{-1}. The purity was determined by A_{260}/A_{280} ratio in a spectrophotometer ELISA reader (Synergy HT microplate reader, Biotek®, USA). Reverse transcription was synthetized by ImProm-II™ Reverse Transcription System (Promega, Madison, WI, USA). To synthesize the cDNA, 2 µg of total cellular RNA was used as templates in a 20 µL reaction containing 1 µL dNTPs (0.5 mM), 1 µL oligo$(dT)_{15}$ primers, 4 µL first strand buffer, 4 µL $MgCl_2$ (8 mM), 0.8 µL RNaseOUT and 200 U ImProm-II™ II reverse transcriptase and nuclease-free water to a final volume of 20 µL, and the reaction was performed at 42 °C for 1 h.

Gene expression using digital PCR

Digital PCR was performed on a QuantStudio™ 3D Digital PCR System platform. Primers and TaqMan®-probes were applied from TaqMan® Assays (Life Technologies): NF-kappa-B: RefSeq NM_001165412.1, ID Hs00765730_m1, IL8: RefSeq NM_000584.3, ID Hs00174103_m1 and COX-2: RefSeq NM000963.3, ID Hs00153133_m1. We prepared 15 µL of reaction mixes containing 7.5 µL QuantStudio™ 3D Digital PCR Master Mix (Life Technologies), 0.7 µL TaqMan® Assay mix, 1.8 µL diluted cDNA (400 ng $µL^{-1}$; 120,000 copies), and 5 µL nuclease-free water. The QuantStudio™ 3D Digital PCR Master Mix contains FAM™ dye. We loaded 15 µL of the reaction mixture onto a QuantStudio™ 3D Digital PCR 20K Chip (Life Technologies). The chip is portioned in 20,000 consistently sized reaction wells. Loaded chips underwent

thermocycling on the ProFlex PCR System under the following conditions: 95 °C for 5 min, 39 cycles at 60 °C for 2 min, and at 72 °C for 2 min. After thermocycling, the chips were imaged on the QuantStudio™ 3D Instrument. QuantStudio™ 3D AnalysisSuite™ Cloud Software was used for quantitative data analysis by Poisson distribution.

DNA copy number determination

In absolute quantification using Digital PCR, no known standards are needed. The target of interest was directly quantified with precision determined by number of digital PCR replicates in the chip. Digital PCR was worked by partitioning a sample into many individual PCR reactions; some portions of these reactions do contain the target molecule (positive), while others do not (negative). Absolute quantification was determined by the numeric ratio of negative versus total reactions. The copy number for NF-κB, COX-2, and IL-8 was determined as previously described methods (Banskota et al. 2015; Regmi et al. 2014; Yun et al. 2006). Copy number of templates was calculated using Eq. (1):

$$\mathrm{DNA(copies)} = \left[6.023 \times 10^{23}\left(\frac{\mathrm{copies}}{\mathrm{mole}}\right) \times \mathrm{DNA\ concentration\ (g)}\right] \div \left[\mathrm{DNA\ length\ (bp)} \times 660\left(\frac{\frac{\mathrm{g}}{\mathrm{mole}}}{\mathrm{bp}}\right)\right] \quad (1)$$

and confirmed with the tool: DNA Copy Number and Dilution Calculator of Applied Biosystems, ThermoFisher Scientific. The resulting data are reported in copies μL^{-1}.

Statistical analysis

Principal component analysis was used to establish the influence of hydroacetonic solutions for the extraction of flavonoids. Correlations between flavonoids were obtained by calculating the Pearson's correlation. Analysis of cell responses were carried out in triplicate and expressed as the mean ± SD. Data were analyzed by one-way ANOVA and differences among treatments were determined by comparison of means using Tukey and Dunnet tests using Statistica v7.2 (StatSoft, Tulsa, OK, USA). The level of statistical significance was considered at $P < 0.05$.

Results

Effect of different hydroacetonic relationships in the extraction of phenolic compounds

There is great interest in the study of biological properties of recognized medicinal plants with the purpose of identifying their active principles and therapeutic functionality. In this study, the influence of different relationships of hydroacetonic solutions on the profile of the main phenolic constituents of *Buddleja scordioides* was characterized, comparing it with the profiles obtained in protic and aprotic conditions. The phenolic profiles identified by LC–ESI–MS/MS demonstrated the presence of 12 phenolic acids and 16 flavonoids (Table 1).

The results indicate that the conditions that favored most the extraction of phenolic acids, was the protic condition (*Inf*), which was characterized by greater abundance of hydroxybenzoic acids, followed by hydroxycinnamic acids. For its part, among the hydroacetonic extractions, the ratio that induced higher content of flavonols was the 85/15 ratio of aqueous acetone (*EAc*) (Fig. 1a). Quercetin is commonly found in its glycosidic form (Fig. 2), therefore in this *EAc*, the main groups of quercetin derivatives found in *Buddleja scordioides* were (Table 1) quercetin 3-O-ß-glucuronide (477→301), isoquercitrin (463→300), rutin (609→300), hyperoside (463→300), and quercetin (301→151). Particularly, under these conditions of extraction (*EAc*), the metabolite detected in the highest concentration was quercetin (259 $\mu g\ g^{-1}$ dry $sample^{-1}$).

For its part, the results of relative abundance obtained with *Inf*, acetone 100% and hydroacetonic solutions [70, 75, 80, 85, 90 and 95% of acetone] were examined using the technique of principal components analysis (Fig. 1b), as it has been used by others to evaluate the effect of solvent (Boeing et al. 2014). Our results indicated that effectively the ratio with 85% acetone was efficient for the extraction of di-hydroxy-flavonoids and some of their glycosidic derivatives; while the use of higher amounts of either acetone or water significantly reduces the extraction of them. Such behavior must be associated with the phenomenon of solubility, which is important to mention that although the solubility is associated with the polarity of solvent and solutes, there are other factors that can affect it; among them are the chemical structure, the functional groups present in the molecules and the solvation effects (Zhang et al. 2015). Besides, the physical state and the presence of other compounds can also affect the solubility. In the present experiment and specifically in the case of flavonols, there is no clear relationship between the solubility and the thermodynamic properties T and ΔH of solubility (Table 2), as it has been documented for the phenolic acids (Gracin and Rasmuson 2002). According to Chebil et al. (2007), such behavior occurs due to the three structural rings and the hydroxyl groups found in flavonols. In this sense, rutin, isoquercitrin, quercetin, among other flavonols, are not planar molecules, since they have a torsion angle of approximately −25°. This magnitude is related to the presence or absence of a double bond between the C2 and the C3, in such a way that the absence of this insaturation in the C ring causes a larger torsion of ~40°, which implies higher solubility in acetonitrile (for example naringenin and

Table 1 Compounds identified in *Buddleja scordioides* by LC–ESI–QqQ

No.	Retention time (min)	Molecular weight	Main transition *m/z*	λmax (nm)	Suggested compounds
1.	6.51	138.12	137.04 > 93.05	320	4-hydroxybenzoic acid (4HB A)[a]
2.	6.62	154.12	153.15 > 108.92	320	Gentisic acid (GA)[a]
3.	6.63	354.31	353.30 > 173.01	320	4-O-Caffeoylquinic acid (4-O-CQA)[a]
4.	6.71	354.31	353.34 > 191.06	320	5-O-Caffeoylquinic acid (5-O-CQA)[a]
5.	7.30	168.14	167.18 > 123.09	320	Vanillic acid (VA)[a]
6.	7.31	180.16	179.19 > 135.08	320	Caffeic acid (CaA)[a]
7.	7.57	198.17	197.21 > 153.11	320	Syringic acid (SA)[a]
8.	8.27	154.12	153.15 > 153.52	320	2,4,6-trihydroxybenzaldehyde (2,4,6 THBa)[a]
9.	8.29	478.36	477.26 > 301.10	375	Quercetin 7-O-ß-Glucuronide (Q7OßG)[a]
10.	8.38	464.38	463.36 > 300.42	375	Hyperoside (Hy)[b]
11.	8.53	164.04	163.24 > 119.08	320	Coumaric acid (CA)[a]
12.	8.76	610.51	609.28 > 300.24	375	Rutin (R)[a]
13.	8.92	224.21	223.24 > 149.04	320	Sinapic acid (SiA)[a]
14.	8.93	464.38	463.36 > 300.42	375	Isoquercitrin (IQ)[a]
15.	8.98	462.36	461 > 285	280	Luteolin 7-O-glucuronide (L7OG)[b]
16.	9.08	194.18	193.24 > 134.04	320	Ferulic acid (FA)[a]
17.	9.68	490.18	489 > 285	280	Luteolin 7-O-6″-acetyl hexoside (L7O6″AH)[b]
18.	9.79	476.21	475 > 299	280	Chrysoeriol uronic acid (CUA)[b]
19.	9.92	520.44	519 > 315	280	Isorhamnetin acetyl glucoside (IAG)[b]
20.	10.25	138.12	137.04 > 93.05	320	Salicylic acid (SaA)[a]
21.	10.63	318.23	317.21 > 151.03	375	Myricetin (My)[a]
22.	11.32	286.24	285.21 > 133.04	280	Luteolin (L)[a]
23.	11.40	302.23	301.20 > 151.02	375	Quercetin (Q)[a]
24.	12.29	270.05	269.27 > 117.04	280	Apigenin (A)[a]
25.	12.37	272.25	271.28 > 119.06	280	Naringenin (N)[a]
26.	12.43	328.32	327 > 229	280	Hydroxy tetramethoxyflavone (HTMF)[b]
27.	12.49	286.23	285.22 > 151.02	375	Kaempferol (K)[a]
28.	13.89	330.29	329 > 314	280	Trihydroxy-dimethoxyflavone (THDMF)[b]

[a]Compared to standard

[b]Confirmed by the fragmentation pattern in MS/MS

hesperetin). When the double bond is present (e.g., rutin, isoquercitrin, and quercetin) the solubility in acetone is favored, while becoming highly insoluble in acetonitrile or water (Chebil et al. 2010).

In addition, in the specific case of quercetin, different solvation patterns have been documented with the hydroxyl groups present in C3', C4', and C7, depending on the solvent used, causing differences in solubility. It is important to point out that thementioned studies were carried out in model systems and that in the case of the present experiment when trying to model the solubility of flavonols in hydroacetonic solutions in different conditions at 313.15 K, they showed greater theoretical solubility in acetone 100%. It was used the Marrero and Gani model (2001) to obtain the temperature and melting enthalpy, as well as the modified UNIFAC method to estimate the activity coefficients according to the methodology of Theo et al. (2016), obtaining the solubility by means of Eq. (2):

$$Ln\, x\gamma = -\left[\frac{\Delta Hm}{RT}\right] \times \left[1 - \frac{T}{Tm}\right], \tag{2}$$

where x is the molar fraction of the solute, γ is the activity coefficient of the solute, which is the result of the residual and combinatorial coefficients shown in Table 2; ΔHm is the enthalpy of fusion, R is the universal gas constant, T is the temperature in Kelvin degrees, and Tm is the melting temperature of the solute in Kelvin degrees.

According to the results obtained, it was found that the use of mixtures of organic solvents with water was more efficient in the extraction of polyphenols. Similar results have been documented by Dent et al. (2013), who found that glycosidic phenolic acids and flavones were more efficiently extracted using 30% aqueous acetone. Furthermore, Ismail et al. (2019) demonstrated through studies by

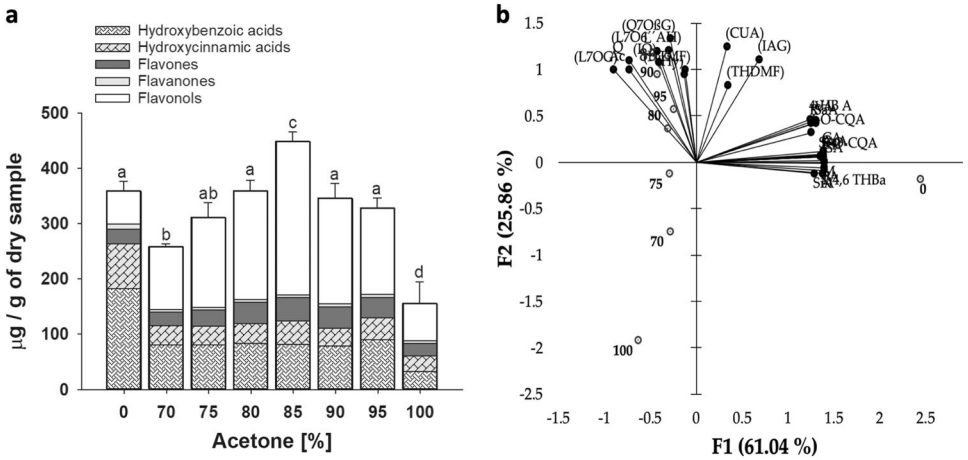

Fig. 1 Effect of the solvent ratio on the extraction of phenolic compounds. **a** Content of different phenolic suclases and **b** PCA plot of the relationships variables (infusion 0% of acetone, acetone 100%, and hydroacetonic solutions [70, 75, 80, 85, 90, and 95% of acetone]) and attributes (flavonol and flavone derivatives, flavanone). Active variables are denoted with black circles and active observations with white circles. The data represents the average of three replicates

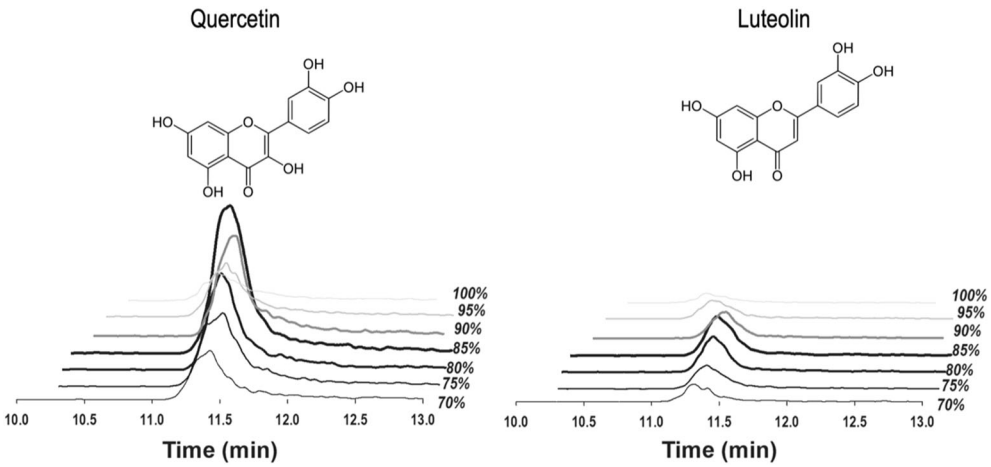

Fig. 2 Representative chromatograms of quercetin and luteolin at next hydroacetonic solutions 70, 75, 80, 85, 90, 95, and 100% of acetone and their chemical structures

LC–MS/QTOF in fruit pulp of baobab that the best extraction condition of those used in its experimental strategy (acetone, methanol, and water in different proportions) was 80% acetone, a condition very close to that obtained in the present experiment. Although from the solubility theory of Hildebrand (1981), the use of acetone favors the extraction of flavonols (Table 2) and the addition of a slight amount of water into the solution causes an increase in the amount of OH interactions. The latter in presence of glycosylated compounds, favors their extraction. For aglycone compounds (quercetin for example), water causes a swelling in the physical structure of the material, where polyphenol is occluded, favoring chemical interactions that allows an increase in the solubility according to the chemical structure and the functional groups present in the bioactive compounds. It is important to consider the suitable proportion of water to use, since a greater amount of it in the mixture would cause a greater swelling, but a smaller amount of interactions, decreasing its solubility. On the contrary, a smaller amount of water will cause a lower degree of swelling, making only polyphenols closer to the solvent to be dragged, leaving an amount without access to the solvent (acetone) due to lack of swelling (little water), thereby decreasing its extraction.

Cell proliferation assay

It is noteworthy to mention that the most important mechanism of di-hydroxy-flavonoids as quercetin and luteolin and some of their glycosidic derivatives is attributed to their antioxidant and anti-inflammatory activities. Based on the above considerations, we have proposed a cellular model of human intestinal cells, to evaluate the protective capacity of polyphenols in *Buddleja scordioides*. Firstly, we determine the range of concentrations to assess the herbal infusion, which did not affect the cellular environment. We examine a working concentration range (5–100 ng mL^{-1} of lyophilized *Inf* and *EAc*) that ensured

Table 2 Thermodynamic parameters of solubility of the compounds identified in *Buddleja scordioides*

No.	Compound	T fusion parameters	ΔH fusion	Parameters for calculating the activity coefficients							
1	4HB A	Tf = 147.45	Hctrl = 2.806	aCH	COOH	OH				Acetone	Water
		COOH = 7.404	COOH = 10.692	Rk = 0.948	Rk = 1.431	Rk = 0.948				Rk = 0.371	Rk = 0.9
		OH = 2.788	OH = 4.786	Qk = 0.774	Qk = 1.214	Qk = 0.893				Qk = 0.109	Qk = 1.4
		aCH = 0.586	aCH = 1.948								
2	GA	Tf = 147.45	Hctrl = 2.806	aCH	COOH	OH				Acetone	Water
		COOH = 7.4042	COOH = 10.692	Rk = 0.948	Rk = 1.431	Rk = 2 × 0.948				Rk = 0.371	Rk = 0.9
		OH = 2 × 2.788	OH = 2 × 4.786	Qk = 0.774	Qk = 1.214	Qk = 2 × 0.893				Qk = 0.109	Qk = 1.4
		aCH = 0.586	aCH = 1.948								
3	4-O-CQA	Tf = 147.45	Hctrl = 2.806	aCH	COOH	OH	HCOO			Acetone	Water
		aCH = 2 × 0.586	aCH = 2 × 1.948	Rk = 2 × 0.948	Rk = 1.431	Rk = 7 × 0.9488	Rk = 3 × 1.229			Rk = 0.371	Rk = 0.9
		OH = 7 × 2.788	OH = 7 × 4.786	Qk = 2 × 0.774	Qk = 1.214	Qk = 7 × 0.8932	Qk = 3 × 1.188			Qk = 0.109	Qk = 1.4
		COOH = 7.404	COOH = 10.692								
		HCOO = 3 × 2.022	HCOO = 3 × 8.11								
4	5-O-CQA	Tf = 147.45	Hctrl = 2.806	aCH	COOH	OH	HCOO			Acetone	Water
		aCH = 2 × 0.586	aCH = 2 × 1.948	Rk = 2 × 0.948	Rk = 1.431	Rk = 7 × 0.948	Rk = 3 × 1.229			Rk = 0.371	Rk = 0.9
		OH = 7 × 2.788	OH = 7 × 4.786	Qk = 2 × 0.774	Qk = 1.214	Qk = 7 × 0.893	Qk = 3 × 1.188			Qk = 0.109	Qk = 1.4
		COOH = 7.404	COOH = 10.692								
		HCOO = 3 × 2.0223	HCOO = 3 × 8.11								
5	VA	Tf = 147.45	Hctrl = 2.806	aCH	COOH	OH		OCH3		Acetone	Water
		COOH = 7.404	COOH = 10.692	Rk = 0.948	Rk = 1.431	Rk = 0.948		Rk = 1.179		Rk = 0.371	Rk = 0.9
		aCH = 0.586	aCH = 1.948	Qk = 0.774	Qk = 1.214	Qk = 0.893		Qk = 0.979		Qk = 0.109	Qk = 1.4
		OH = 2.788	OH = 4.786								
		OCH3 = 5.089	OCH3 = 5.089								
6	CaA	Tf = 147.45	Hctrl = 2.806	aCH	COOH	OH			C=C	Acetone	Water
		OH = 2 × 2.788	OH = 2 × 4.786	Rk = 0.948	Rk = 1.431	Rk = 2 × 0.948			Rk = 0.660	Rk = 0.371	Rk = 0.9
		COOH = 7.404	COOH = 10.692	Qk = 0.774	Qk = 1.214	Qk = 2 × 0.893			Qk = 0.408	Qk = 0.109	Qk = 1.4
		C=C = 0.392	C=C = 2.616								
		aCH = 0.586	aCH = 1.948								
7	SA	Tf = 147.45	Hctrl = 2.806	aCH	COOH	OH		OCH3		Acetone	Water
		OH = 2.7888	OH = 4.786	Rk = 0.948	Rk = 1.431	Rk = 0.948		Rk = 2 × 1.179		Rk = 0.371	Rk = 0.9
		COOH = 7.404	COOH = 10.692	Qk = 0.774	Qk = 1.214	Qk = 0.893		Qk = 2 × 0.979		Qk = 0.109	Qk = 1.4
		OCH3 = 2 × 5.089	OCH3 = 2 × 5.089								
		aCH = 0.586	aCH = 1.948								
8	2,4,6 THBa	Tf = 147.45	Hctrl = 2.806	aCH		OH				Acetone	Water
		OH = 2 × 2.788	OH = 4 × 4.786	Rk = 0.948		Rk = 4 × 0.948				Rk = 0.371	Rk = 0.9
		aCH = 0.586	aCH = 1.98	Qk = 0.774		Qk = 4 × 0.893				Qk = 0.109	Qk = 1.4
9	Q7OßG	Tf = 147.45	Hctrl = 2.806	aCH	COOH	OH				Acetone	Water
		aCH = 3 × 0.586	aCH = 3 × 1.98	Rk = 3 × 0.948	Rk = 1.431	Rk = 8 × 0.948				Rk = 0.371	Rk = 0.9
		OH = 8 × 2.788	OH = 8 × 4.786	Qk = 3 × 0.774	Qk = 1.214	Qk = 8 × 0.893				Qk = 0.109	Qk = 1.4

Table 2 (continued)

No.	Compound	T fusion parameters	ΔH fusion	Parameters for calculating the activity coefficients						
		COOH = 7.404 aC–O = 5.147	COOH = 10.692 aC–O = −0.118				aC–O Rk = 0.609	aC–CO Rk = 1.022		
		aC–CO = 12.429	aC–CO = 8.149				Qk = 0.360	Qk = 0.836		
10	Hy	Tf = 147.45	Hctrl = 2.806	aCH		OH			Acetone	Water
		aCH = 4 × 0.586	aCH = 4 × 1.98	Rk = 4 × 0.948		Rk = 8 × 0.948			Rk = 0.371	Rk = 0.9
		OH = 8 × 2.788	OH = 8 × 4.786	Qk = 4 × 0.774		Qk = 8 × 0.893			Qk = 0.109	Qk = 1.4
		aC–O = 5.147	aC–O = −0.118				aC–O	aC–CO		
		aC–CO = 2 × 12.429	aC–CO = 2 × 8.149				Rk = 0.609	Rk = 2 × 1.022		
							Qk = 0.360	Qk = 2 × 0.836		
11	CA	Tf = 147.45	Hctrl = 2.806	aCH	COOH	OH			Acetone	Water
		COOH = 7.404	COOH = 10.692	Rk = 0.948	Rk = 1.431	Rk = 0.948			Rk = 0.371	Rk = 0.9
		OH = 2.788	OH = 4.786	Qk = 0.774	Qk = 1.214	Qk = 0.893			Qk = 0.109	Qk = 1.4
		CH2=C = 2.451	CH2=C = 2.451							
		aCH = 0.586	aCH = 1.98							
12	R	Tf = 147.45	Hctrl = 2.806	aCH		OH			Acetone	Water
		aCH = 5 × 0.586	aCH = 5 × 1.98	Rk = 5 × 0.948		Rk = 10 × 0.948			Rk = 0.371	Rk = 0.9
		OH = 10 × 2.788	OH = 10 × 4.786	Qk = 5 × 0.774		Qk = 10 × 0.893	aC–O	aC–CO	Qk = 0.109	Qk = 1.4
		aC–O = 4 × 5.147	aC–O = 4 × −0.118				Rk = 4 × 0.609	Rk = 1.022		
		aC–CO = 12.429	aC–CO = 8.149				Qk = 4 × 0.360	Qk = 0.836		
13	SiA	Tf = 147.45	Hctrl = 2.806	aCH	COOH		OCH3	C=C	Acetone	Water
		COOH = 7.404	COOH = 10.692	Rk = 0.948	Rk = 1.431		Rk = 2 × 1.179	Rk = 0.660	Rk = 0.371	Rk = 0.9
		OCH3 = 2 × 2.022	OCH3=2 × 5.089	Qk = 0.774	Qk = 1.214		Qk = 2 × 0.979	Qk = 0.408	Qk = 0.109	Qk = 1.4
		C=C = 0.392	C=C = 6.128							
		aCH = 0.586	aCH = 1.98							
14	IQ	Tf = 147.45	Hctrl = 2.806	aCH		OH			Acetone	Water
		aCH = 4 ×0.586	aCH = 4 × 1.98	Rk = 4 × 0.948		Rk = 8 × 0.948			Rk = 0.371	Rk = 0.9
		OH = 8 × 2.788	OH = 8 × 4.786	Qk = 4 × 0.774		Qk = 8 × 0.893	aC–O	aC–CO	Qk = 0.109	Qk = 1.4
		aC–O = 3 ×5.147	aC–O = 3 × −0.118				Rk = 3 × 0.609	Rk = 1.022		
		aC–CO = 12.429	aC–CO = 8.149				Qk = 3 × 0.360	Qk = 0.836		
15	L7OG	Tf = 147.45	Hctrl = 2.806	aCH					Acetone	Water
		aCH = 4 × 0.586	aCH = 4 × 1.98	Rk = 4 × 0.948			aC–O	aC–CO	Rk = 0.371	Rk = 0.9
		aC–O = 2 × 5.147	aC–O = 2 × −0.118	Qk = 4 × 0.774			Rk = 2 × 0.609	Rk = 1.022	Qk = 0.109	Qk = 1.4
		aC–CO = 12.429	aC–CO = 8.149				Qk = 2 × 0.360	Qk = 0.836		
16	FA	Tf = 147.45	Hctrl = 2.806	aCH	COOH	OH	OCH3	C=C	Acetone	Water
		OH = 2 × 2.788	OH = 2 × 4.786	Rk = 0.948	Rk = 1.431	Rk = 2 × 0.948	Rk = 1.179	Rk = 0.660	Rk = 0.371	Rk = 0.9
		COOH = 7.404	COOH = 10.692	Qk = 0.774	Qk = 1.214	Qk = 2 × 0.893	Qk = 0.979	Qk = 0.408	Qk = 0.109	Qk = 1.4
		OCH3 = 1 × 2.0223	OCH3 = 1 × 5.089							
		aCH = 0.586	aCH = 1.98					aC–CO		
		C=C = 0.392	C=C = 6.128					Rk = 1.022		
		aC–CO = 12.429	aC–CO = 8.149					Qk = 0.836		

Table 2 (continued)

No.	Compound	T fusion parameters	ΔH fusion	Parameters for calculating the activity coefficients						
17	L7O6´´AH	Tf = 147.45	OH = 7 × 4.786	aCH		OH			Acetone	Water
		OH = 7 × 2.788	aCH = 4 × 1.98	Rk = 4 × 0.948		Rk = 7 × 0.948	aC–O		Rk = 0.371	Rk = 0.9
		aCH = 4 × 0.586	aC–O = 3 × −0.118	Qk = 4 × 0.774		Qk = 7 × 0.893	Rk = 0.609		Qk = 0.109	Qk = 1.4
		aC–O = 3 × 5.147					Qk = 0.360			
18	CUA	Tf = 147.45	Hctrl = 2.806	aCH	COOH	OH			Acetone	Water
		OH = 2 × 2.788	OH = 7 × 4.786	Rk = 3 × 0.948	Rk = 1.431	Rk = 7 × 0.948			Rk = 0.371	Rk = 0.9
		aCH = 3 × 0.586	aCH = 3 × 1.98	Qk = 3 × 0.774	Qk = 1.214	Qk = 7 × 0.893	aC–O		Qk = 0.109	Qk = 1.4
		aC–O = 5.147	aC–O = −0.118				Rk = 0.609			
		COOH = 7.404	COOH = 10.692				Qk = 0.360			
19	IAG	Tf = 147.45	Hctrl = 2.806	aCH		OH			Acetone	Water
		aCH = 4 × 0.586	aCH = 4 × 1.98	Rk = 4 × 0.948		Rk = 7 × 0.948			Rk = 0.371	Rk = 0.9
		OH = 7 × 2.788	OH = 7 × 4.786	Qk = 4 × 0.774		Qk = 7 × 0.893	aC–O	aC–CO	Qk = 0.109	Qk = 1.4
		aC–O = 5.147	aC–O = −0.118				Rk = 0.609	Rk = 1.022		
		aC–CO = 12.429	aC–CO = 8.149				Qk = 0.360	Qk = 0.836		
20	SaA	Tf = 147.45	Hctrl = 2.806	aCH	COOH	OH			Acetone	Water
		aCH = 0.586	aCH = 1.98	Rk = 0.948	Rk = 1.431	Rk = 0.948			Rk = 0.371	Rk = 0.9
		OH = 2.788	OH = 4.786	Qk = 0.774	Qk = 1.214	Qk = 0.893			Qk = 0.109	Qk = 1.4
		COOH = 7.404	COOH = 10.692							
21	My	Tf = 147.45	Hctrl = 2.806	aCH		OH			Acetone	Water
		aCH = 3 × 0.586	aCH = 3 × 1.98	Rk = 3 × 0.948		Rk = 6 × 0.948			Rk = 0.371	Rk = 0.9
		OH = 6 × 2.788	OH = 6 × 4.786	Qk = 3 × 0.774		Qk = 6 × 0.893	aC–O	aC–CO	Qk = 0.109	Qk = 1.4
		aC–O = 5.147	aC–O = −0.118				Rk = 0.609	Rk = 1.022		
		aC–CO = 12.429	aC–CO = 8.149				Qk = 0.360	Qk = 0.836		
22	L	Tf = 147.45	Hctrl = 2.806	aCH		OH			Acetone	Water
		aCH = 3 × 0.586	aCH = 3 × 1.98	Rk = 3 × 0.948		Rk = 4 × 0.948			Rk = 0.371	Rk = 0.9
		OH = 4 × 2.788	OH = 4 × 4.786	Qk = 3 × 0.774		Qk = 4 × 0.893	aC–O	aC–CO	Qk = 0.109	Qk = 1.4
		aC–O = 5.147	aC–O = −0.118				Rk = 0.609	Rk = 1.022		
		aC–CO = 12.429	aC–CO = 8.149				Qk = 0.360	Qk = 0.836		
23	Q	Tf = 147.45	Hctrl = 2.806	aCH		OH			Acetone	Water
		aCH = 3 × 0.586	aCH = 3 × 1.98	Rk = 3 × 0.948		Rk = 5 × 0.948			Rk = 0.371	Rk = 0.9
		OH = 5 × 2.788	OH = 5 × 4.786	Qk = 3 × 0.774		Qk = 5 × 0.893	aC–O	aC–CO	Qk = 0.109	Qk = 1.4
		aC–O = 5.147	aC–O = −0.118				Rk = 0.609	Rk = 1.022		
		aC–CO = 12.429	aC–CO = 8.149				Qk = 0.360	Qk = 0.836		
24	A	Tf = 147.45	Hctrl = 2.806	aCH		OH			Acetone	Water
		aCH = 3 × 0.586	aCH = 3 × 1.98	Rk = 3 × 0.948		Rk = 3 × 0.948			Rk = 0.371	Rk = 0.9
		OH = 3 × 2.788	OH = 3 × 4.786	Qk = 3 × 0.774		Qk = 3 × 0.893	aC–O	aC–CO	Qk = 0.109	Qk = 1.4
		aC–O = 5.147	aC–O = −0.118				Rk = 0.609	Rk = 1.022		
		aC–CO = 12.429	aC–CO = 8.149				Qk = 0.360	Qk = 0.836		
25	N	Tf = 147.45	Hctrl = 2.806	aCH		OH			Acetone	Water
		aCH = 3 × 0.586	aCH = 3 × 1.98	Rk = 3 × 0.948		Rk = 3 × 0.948		aC–CO	Rk = 0.371	Rk = 0.9

Table 2 (continued)

No.	Compound	T fusion parameters	ΔH fusion	Parameters for calculating the activity coefficients						
		OH = 3 × 2.788	OH = 3 × 4.786	Qk = 3 × 0.774	Qk = 3 × 0.893			Rk = 1.022	Qk = 0.109	Qk = 1.4
		aC–CO = 12.429	aC–CO = 8.149					Qk = 0.836		
26	HTMF	Tf = 147.45	Hctrl = 2.806	aCH	OH				Acetone	Water
		aCH = 3 × 0.586	aCH = 3 × 1.98	Rk = 3 × 0.948	Rk = 0.948				Rk = 0.371	Rk = 0.9
		OH = 2.788	OH = 4.786	Qk = 3 × 0.774	Qk = 0.893				Qk = 0.109	Qk = 1.4
		aC–OH = 4 × 8.427	aC–OH = 4 × 8.427							
27	K	Tf = 147.45	Hctrl = 2.806	aCH	OH				Acetone	Water
		aCH = 3 × 0.586	aCH = 3 × 1.98	Rk = 3 × 0.948	Rk = 4 × 0.948				Rk = 0.371	Rk = 0.9
		OH = 4 × 2.788	OH = 4 × 4.786	Qk = 3 × 0.774	Qk = 4 × 0.893	aC–O		aC–CO	Qk = 0.109	Qk = 1.4
		aC–O = 5.147	aC–O = −0.118			Rk = 0.609		Rk = 1.022		
		aC–CO = 12.429	aC–CO = 8.149			Qk = 0.360		Qk = 0.836		
28	THDMF	Tf = 147.45	Hctrl = 2.806	aCH	OH	OCH3			Acetone	Water
		aCH = 3 × 0.586	aCH = 3 × 1.98	Rk = 3 × 0.948	Rk = 3 × 0.948	Rk = 1.179			Rk = 0.371	Rk = 0.9
		OH = 3 × 2.788	OH = 3 × 4.786	Qk = 3 × 0.774	Qk = 3 × 0.893	Qk = 0.979			Qk = 0.109	Qk = 1.4
		OCH3 = 1 × 2.022	OCH3 = 1 × 5.089							
		aC–O = 5.147	aC–O = −0.118			aC–O		aC–CO		
		aC–CO = 12.429	aC–CO = 8.149			Rk = 0.609		Rk = 1.022		
						Qk = 0.360		Qk = 0.836		

the no toxicity condition into the cellular environment. Particularly, the extractables evaluated showed no toxic effects at concentrations of 100 ng mL^{-1} compared with the control without treatment.

Intracellular ROS measurement

ROS, such as hydrogen peroxide (H_2O_2), hydroxyl radical (OH·), and superoxide (O^{2-}) are produced in mammalian cells as a result of normal metabolism due to activation of enzymes in response to different stimuli in several pathways. The presence of H_2O_2 in the cells, foment one-electron oxidation of H_2DCF, promoting the formation of dichlorofluorescein (DCF), which is a product highly fluorescent and capable of being detected by flow cytometry. To determine whether *B. scordioides* treatment can attenuate oxidative stress in colon cancer cells, HT-29 cells were treated with 400 mM of H_2O_2 for 1 h and incubated with H_2DCF-DA. Then, the attenuation of ROS was examined by measuring the cells population with positive DCF-derived from H_2O_2 treatment after the *B. scordioides* treatment. Data analysis was done with the FlowJo V10 software comparing the fluorescence in a gate defined for all treatments and controls.

The cells not subjected to stress induction with H_2O_2 showed a basal level of DCF. In the cells subjected to oxidative stress with H_2O_2, the fluorescence increased from 43% in positive control cells (Fig. 3e), compared with the levels shown by the control without stress induction by H_2O_2. To demonstrate the antioxidant effect of the *B. scordioides* extracts, it was compared the intensity of fluorescence emitted by cells treated at 100 ng mL^{-1} of *Inf* and *EAc* of *B. scordioides*, followed by the induction of ROS with H_2O_2 to a single dose.

Effect of infusion and hydroacetonic extracts in the anti-inflammatory process

In the colon, inflammation causes an increase in the permeability of the epithelium allowing the entry of Ca^{2+} ions into the cell cytoplasm. The increase of intracellular Ca^{2+} causes the activation of kinase C protein, which activates directly to NF-κB. The activation of NF-κB is related to increased expression of COX-2 and IL-8. In this paper, we investigated the effect of *Inf* and *EAc* on three inflammation markers: NF-κB, COX-2, and IL-8 as indicative of functionality in anti-inflammatory tests covering the main activation pathways of intestinal inflammation (Fig. 4). Due to the importance that NF-κB and IL-8 have during inflammation, they have become diagnostic markers of inflammation. In addition, IL-8 is used as a positive control in studies of inflammation of the colon.

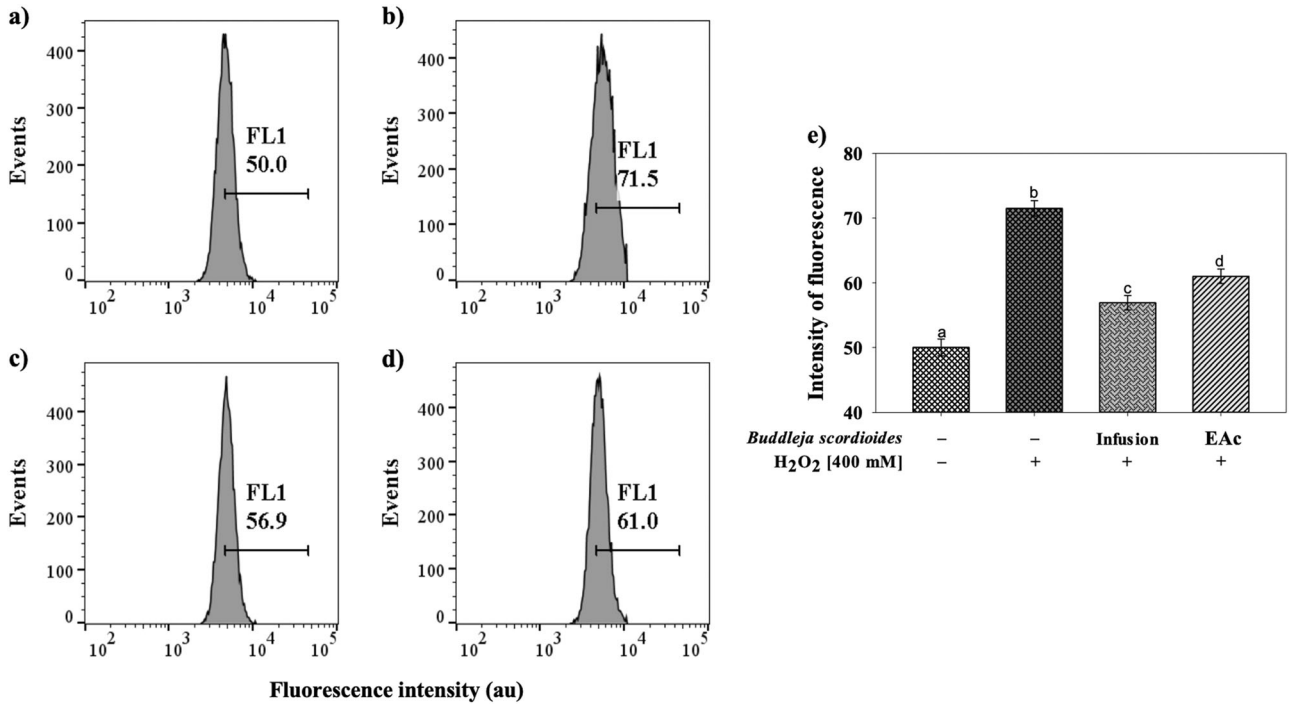

Fig. 3 Effect of *Buddleja scordioides* extracts against oxidative stress induced with H_2O_2. **a** Negative control (Control), cells treated with DMSO (0.04%) as vehicle; **b** positive control (Control H_2O_2), cells treated with H_2O_2 for 1 h without salvilla treatment; **c** cells pretreated 24 h with *Inf* at 100 ng/mL and cotreated with H_2O_2 for 1 h; **d** cells pretreated 24 h with acetone extracts (85%) of *Buddleja scordioides* at 100 ng/mL and cotreated with H_2O_2 for 1 h; **e** fluorescence intensity of *Buddleja scordioides* infusion, extract, positive and negative controls fluorescence. Data are expressed as the mean value ± SD of three experiments; different letters represent significant difference versus control (Tukey, $p < 0.05$). au denote arbitrary units of fluorescence intensity

Previous studies demonstrated by computational analysis the binding affinity patterns between flavonoids and the COX-2 enzyme (Dash et al. 2015), where they found several structural characteristics that are considered important for the efficient inhibition of COX. An important aspect for the development of selective COX-2 drugs is partly due to a polar hydrophilic side-pocket that is formed by the substitution of COX-1 amino acids different from those substituted in COX-2. This causes the volume of the active site of COX-2 to increase and allows these isoenzymes to bind bulky inhibitors more rapidly than COX-1. Flavonoids such as 4',6,7-tri-hydroxy-isoflavone, quercetin, quercetin-3-methyl ether, kaempferol, and luteolin bind favorably to the active site of COX-2 and are therefore considered potential candidates for studies aimed at the treatment of inflammation. In this investigation we found that *Inf* and *EAc* decrease the number of COX-2 transcripts in colon epithelial cells with inflammation induced by LPS (Fig. 3a). The possible mechanism of action of the polyphenols present in *inf* and *EAc* can be attributed to their ability to recognize the active site of COX-2 and to the difference in the content of compounds between the infusion and *EAc*. Among the compounds present abundantly in *B. scordioides* is luteolin. Luteolin is a di-hydroxy-flavonoid highly studied for its reports as a suppressor of COX-2 expression in colon cancer, as well as in noncancer cells. There is also information that supports the low toxicity of luteolin in normal cells. Besides, it is relevant to mention that these compounds in a pure state are less effective than in a matrix composed of flavonoids, phenolic acids, and other phytochemical compounds, for this reason it is relevant to characterize and optimize the selectivity of the compounds present in plant extracts for their use as nutraceuticals.

Phytochemical compounds are well known for their high reactivity with proteins. This property is very important during the cell signaling process due to the alteration of molecular mechanisms by the interaction with genes and proteins that regulate their expression. In this context, the aryl hydrocarbon receptor (AhR) is a transcription factor that regulates the expression of genes, one of its functions is as a sensor of chemical xenobiotics and their metabolism (Xue et al. 2017). The AhR binds to exogenous ligands such as polyphenols, flavonoids, and polycyclic aromatic hydrocarbons. During its activation, it first binds with the AhR nuclear translocator protein (ARNT) and is activated through the formation of the heteromeric complex (AhR/ARNT), then the AhR/ARNT is able to directly or indirectly interact with the DNA by binding to recognition sequences located in the 5' regulatory region of the inducible genes. Potapovich

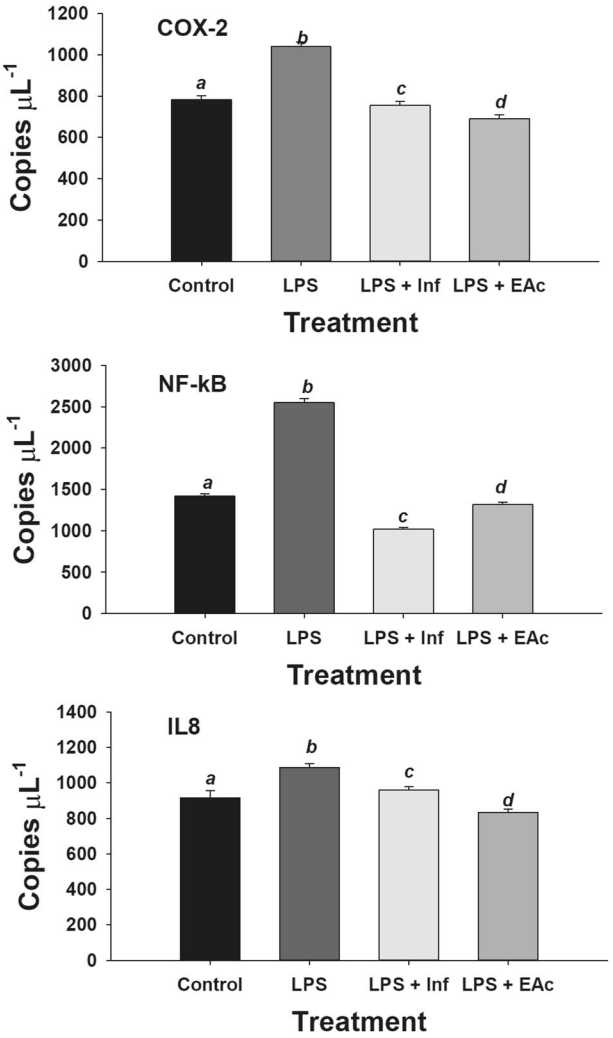

Fig. 4 Expression of inflammatory genes in HT-29 cells subjected to inflammation with LPS and treated with *Inf* and *EAc* of *Buddleja scordioides*. Quantification of DNA copy numbers in cells was analyzed in 3D dPCR Chip. Chip data were analyzed with QuantStudio™ 3D AnalysisSuite™ Cloud Software for quantitative data analysis

et al. (2011) demonstrated that flavonols such as quercetin differentially modulate the inflammatory response in human cells through various signal transduction pathways including AhR. A key factor in the demonstration of activity of polyphenols during the modulation of inflammation depends on the phenolic nucleus, its structure and its glycosylation. The participation of AhR in the synthesis de novo of IL-8 has been demonstrated by specific methods of anti-AhR with small interfering RNA. Our results show a decrease in the amount of NF-κB transcripts with a possible mechanism of inhibition of active NF-κB (Fig. 4b), so it is expected that IL-8 will also be diminished. However, our results show an increase in IL-8 in colon cells coincubated with LPS and infusions (Fig. 3c). With these results we conclude that the initial inhibitory phase was independent of AhR and was a response to the initial and temporary phosphorylation of redox p65, while the late regulation depended strictly on the activation of AhR. This confirms the reports suggesting that glycosylated compounds isolated mainly in aqueous solutions influence the expression of IL-8 induced by TNF-α in the NF-κB pathway as a mechanism of inflammation (Szczuka et al. 2019). It also approves the suggestion that polyphenols act as inducer and effector of IL-8 synthesis in normal human cells by functional activation of AhR.

Conclusions

In summary, the wide variety of polyphenols in plants implies the need to establish an effective methodology for efficient extraction and characterization. Hydroacetonic mixtures improve the concentration of bioactive compounds with energetic stability that allows cellular interactions with antioxidant and anti-inflammatory responses.

Acknowledgements Funding from the Strengthening and Development of Scientific and Technological Infrastructure program (Grants numbers 253333, 280172, and 224651) from the Mexican Science and Technology Council (CONACyT) is recognized. Financial support from TecNM/Instituto Tecnológico de Durango (Grant No. 5557.15) is also acknowledged. Authors CV-N and KMH-R are thankful for graduate scholarships granted by CONACyT for PhD studies.

Compliance with ethical standards

Conflict of interest The authors declare that they have no conflict of interest.

Publisher's note Springer Nature remains neutral with regard to jurisdictional claims in published maps and institutional affiliations.

References

Atala E, Fuentes J, Wehrhahn MJ, Speisky H (2017) Quercetin and related flavonoids conserve their antioxidant properties despite undergoing chemical or enzymatic oxidation. Food Chem 234:479–485

Avila JG, Romo de Vivar A (2002) Triterpenoid saponins and other glycosides from *Buddleja scordioides*. Biochem Syst Ecol 10:1003–1005

Bai X, Liu S, Liu J, Ma Y, Zhang W, Pan J (2018) Specific uptake luteolin by boronate affinity-based single-hole hollow imprinted polymers sealed in dialysis bags. Chem Eng J 353:911–191

Banskota S, Regmi SC, Kim JA (2015) NOX1 to NOX2 switch deactivates AMPK and induces invasive phenotype in colon cancer cells through overexpression of MMP-7. Mol Cancer 14:123–134

Boeing JS, Barizão ÉO, e Silva BC, Montanher PF, de Cinque Almeida V, Visentainer JV (2014) Evaluation of solvent effect on the extraction of phenolic compounds and antioxidant capacities from the berries: application of principal component analysis. Chem Cent J 8:48–49

Chebil L, Chipot C, Archambault F, Humeau C, Engasser JM, Ghoul M, Dehez F (2010) Solubilities inferred from the combination of

experiment and simulation. Case study of quercetin in a variety of solvents. J Phys Chem B 114:12308–12313
Chebil L, Humeau C, Anthoni J, Dehez F, Engasser JM, Ghoul M (2007) Solubility of flavonoids in organic solvents. J Chem Eng Data 52:1552–1556
Choi JS, Islam MN, Ali MY, Kim YM, Park HJ, Sohn HS, Jung HA (2014) The effects of C-glycosylation of luteolin on its antioxidant, anti-Alzheimer's disease, anti-diabetic, and anti-inflammatory activities. Arch Pharm Res 37:1354–1363
Dash R, Uddin MM, Hosen SM, Rahim ZB, Dinar AM, Kabir MS, Sultan RA, Islam A, Hossain MK (2015) Molecular docking analysis of known flavonoids as duel COX-2 inhibitors in the context of cancer. Bioinformation 11:543–549
Dent M, Dragovic-Uzelac V, Penic M, Brncic M, Bosiljkov T, Levaj B (2013) The effect of extraction solvents, temperature and time on the composition and mass fraction of polyphenols in Dalmatian wild sage (*Salvia officinalis* L.) extracts. Food Technol Biotechnol 51:84–91
Díaz-Rivas JO, González-Laredo RF, Chávez-Simental JA, Montoya-Ayón JB, Moreno-Jiménez MR, Gallegos-Infante JA, Rocha-Guzmán NE (2018) Comprehensive characterization of extractable phenolic compounds by UPLC-PDA-ESI-QqQ of *Buddleja scordiodes* plants elicited with salicylic acid. J Chem. https://doi.org/10.1155/2018/4536970
Díaz-Rivas JO, Herrera-Carrera E, Gallegos-Infante JA, Rocha-Guzmán NE, González-Laredo RF, Moreno-Jiménez MR, Ramos-Gómez M, Reynoso-Camacho R, Larrosa-Pérez M, Gallegos-Corona MA (2015) Gastroprotective potential of *Buddleja scordioides* Kunth Scrophulariaceae infusions; effects into the modulation of antioxidant enzymes and inflammation markers in an in vivo model. J Ethnopharmacol 169:280–286
Gracin S, Rasmuson ÅC (2002) Solubility of phenylacetic acid, p-hydroxyphenylacetic acid, p-aminophenylacetic acid, p-hydroxybenzoic acid, and ibuprofen in pure solvents. J Chem Eng Data 47:1379–1383
Hildebrand JH (1981) A history of solution theory. Annu Rev Phys Chem 32:1–24
Ismail BB, Pu Y, Guo M, Ma X, Liu D (2019) LC-MS/QTOF identification of phytochemicals and the effects of solvents on phenolic constituents and antioxidant activity of baobab (*Adansonia digitata*) fruit pulp. Food Chem 277:279–288
Leopoldini M, Prieto-Pitarch I, Russo N, Toscano M (2004) Structure, conformation, and electronic properties of apigenin, luteolin and taxifolin antioxidants. A first principle theoretical study. J Phys Chem A 108:92–96
Li Y, Soendergaard C, Bergenheim FH, Aronoff DM, Milne G, Riis LB, Seidelin JB, Jensen KB, Nielsen OH (2018) COX-2-PGE2 Signaling Impairs Intestinal Epithelial Regeneration and Associates with TNF Inhibitor Responsiveness in Ulcerative Colitis. EBioMedicine 36:497–507
Marrero J, Gani R (2001) Group-contribution based estimation of pure component properties. Fluid Phase Equilibria 183:183–208
Matsumoto H, Ogura H, Shimizu K, Ikeda M, Hirose T, Matsuura H, Kang S, Takahashi K, Tanaka T, Shimazu T (2018) The clinical importance of a cytokine network in the acute phase of sepsis. Sci Rep 8:13995–14003
Mattia C, Coluzzi F (2005) COX-2 inhibitors: pharmacological data and adverse effects. Minerva Anestesiol 71:461–470
Mueller M, Hobiger S, Jungbauer A (2010) Anti-inflammatory activities of extracts from fruits, herbs and spices. Food Chem 122:987–996
Pakade V, Lindahl S, Chimuka L, Turner C (2012) Molecular imprinted polymers targeting quercetin in high-temperature aqueous solutions. J Chromatogr A 1230:15–23
Potapovich AI, Lulli D, Fidanza P, Kostyuk VA, De Luca C, Pastore S, Korkina LG (2011) Plant polyphenols differentially modulate inflammatory responses of human keratinocytes by interfering with activation of transcription factors NFkB and AhR and EGFR-ERK pathway. Toxicol Appl Pharmacol 255:138–149
Psotová J, Chlopciková S, Miketová P, Hrbác J, Simánex V (2004) Chemoprotective effect of plant phenolics against anthracycline-induced toxicity on rat cardiomyocytes. Part III. Apigenin, Baicalelin, Kaempherol, Luteolin and Quercetin. Phytother Res 18:516–521
Regmi SC, Park SY, Ku SK, Kim JA (2014) Serotonin regulates innate immune responses of colon epithelial cells through Nox2-derived reactive oxygen species. Free Rad Biol Med 69:377–389
Rocha-Guzmán NE, Simental-Mendía LE, Barragán-Zúñiga LJ, Ramírez-España JC, Gallegos-Infante JA, Luján-Mendoza CI, Gamboa-Gómez CI (2018) Effect of *Buddleja scordiodes* K. leaves infusion on lipid peroxidation in mice with ultraviolet light-induced oxidative stress. Med Chem Res 27:2379–2385
Seyedabadi M, Rahimian R, Ghia JE (2018) The role of alpha7 nicotinic acetylcholine receptors in inflammatory bowel disease: involvement of different cellular pathways. Expert Opin Ther Tar. 22:161–176
Szczuka D, Nowak A, Zakłos-Szyda M, Kochan E, Szymańska G, Motyl I, Blasiak J (2019) American Ginseng (Panax quinquefolium L.) as a Source of Bioactive Phytochemicals with Pro-Health Properties. Nutrients. https://doi.org/10.3390/nu11051041
Tanih NF, Ndip RN (2017) The acetone extract of *Sclerocarya birrea* (Anacardiaceae) possesses antiproliferative and apoptotic potential against human breast cancer cell lines (MCF-7). Sci World J. https://doi.org/10.1155/2013/956206
Theo WL, Mustaffa AA, Lim JS (2016) Solubility modelling for phytochemicals of *Misai Kucing* in different solvents. Fluid Phase Equilibria 427:246–258
Xue Z, Li D, Yu W, Zhang Q, Hou X, He Y, Kou X (2017) Mechanisms and therapeutic prospects of polyphenols as modulators of the aryl hydrocarbon receptor. Food Funct 8:1414–1437
Yang Y, Bae WK, Nam S-J, Heong M-H, Zhou R, Park S-Y, Tas I, Hwang Y-H, Park M-S, Chung IJ, Kim KK, Hur J-S, Kim H (2018) Acetonic extracts of the endolichenic fungus EL002332 isolated from *Endocarpon pusillum* exhibits anticancer activity in human gastric cancer cells. Phytomedicine 40:106–115
Yun JJ, Heisler LE, Hwang IIL, Wilkins O, Lau SK, Hyrcza M, Jayabalasingham B, Jin J, McLaurin J, Tsao MS, Der SD (2006) Genomic DNA functions as a universal external standard in quantitative real-time PCR. Nucleic Acids Res 34:e85–e94
Zhang Y, Guo F, Cui Q, Lu M, Song X, Tang H, Li Q (2015) Measurement and correlation of the solubility of vanillic acid in eight pure and water+ ethanol mixed solvents at temperatures from (293.15 to 323.15) K. J Chem Eng Data 61:420–429
Zi J, Peng B, Yan W (2007) Solubilities of rutin in eight solvents at T = 283.15, 298.15, 313.15, 323.15, and 333.15 K. Fluid Phase Equilibria 261(1–2):111–114